

**JAERI-M
89-020**

Characteristics of Edge Localized Mode in JFT-2M H-mode

March 1989

Hiroshi MATSUMOTO, R. J. GOLDSTON*, Akimasa FUNAHASHI,
Katsumichi HOSHINO, Hisato KAWASHIMA, Tomohide KAWAKAMI,
Hikosuke MAEDA, Tohru MATOBA, Toshiaki MATSUDA,
Yukitoshi MIURA, Masahiro MORI, Ichiro NAKAZAWA**,
Kazuo ODAJIMA, Hiroaki OGAWA, Toshihide OGAWA,
Kazumi OHASA, Seio SENGOKU, Teruaki SHOJI, Norio SUZUKI,
Hiroshi TAMAI, Yoshihiko UESUGI, Toshihiko YAMAUCHI,
Takumi YAMAMOTO and Hidewo OHTUKA

JAERI Mレポートは、日本原子力研究所が不定期に公開している研究報告書です。
入手の間合わせは、日本原子力研究所技術情報部情報資料課（〒319-11 茨城県那珂郡東海村）にて、
お申しこしてください。なお、このほかに財団法人原子力弘済会資料センター（〒319-11 茨城県那珂郡
東海村日本原子力研究所内）で複写による実費領布をおこなっております。

JAERI-M reports are issued irregularly.

Inquiries about availability of the reports should be addressed to Information Division Department
of Technical Information, Japan Atomic Energy Research Institute, Tokaimura, Naka gun, Ibaraki
ken 319-11, Japan.

© Japan Atomic Energy Research Institute, 1989

編集兼発行 日本原子力研究所
印 刷 日青工業株式会社

Characteristics of Edge Localized Mode in JFT-2M H-Mode

Hiroshi MATSUMOTO, R.J. GOLDSTON^{*}, Akimasa FUNAHASHI
Katsumichi HOSHINO, Hisato KAWASHIMA, Tomohide KAWAKAMI
Hikosuke MAEDA, Tohru MATOBA, Toshiaki MATSUDA
Yukitoshi MIURA, Masahiro MORI, Ichiro NAKAZAWA^{**}
Kazuo ODAJIMA, Hiroaki OGAWA, Toshihide OGAWA
Kazumi OHASA, Seio SENGOKU, Teruaki SHOJI
Norio SUZUKI, Hiroshi TAMAI, Yoshihiko UESUGI
Toshihiko YAMAUCHI, Takumi YAMAMOTO and Hidewo OHTUKA

Department of Thermonuclear Fusion Research
Naka Fusion Research Establishment
Japan Atomic Energy Research Institute
Naka-machi, Naka-gun, Ibaraki-ken

(Received February 1, 1989)

Characteristics of edge localized mode (ELM/ERP) during H-mode plasma of JFT-2M were investigated. It was found that ELM/ERP is mainly a density fluctuation phenomena in the edge, and electron temperature in the edge except just near the separatrix is not very much perturbed. Several experimental conditions to controll ELM/ERP are, plasma density, plasma ion species, heating power, and plasma current ramping. ELM/ERPs found in low density deuterium discharge are suppressed by raising the density. ELM/ERPs are pronounced in hydrogen plasma compared with deuterium plasma. ELM/ERPs seen in hydrogen plasma or in near marginal

Keywords: H-mode, JFT-2M, ELM/ERP, Magnetic Fluctuations

* Princeton Plasma Physics Laboratory, Princeton University

** on leave from Mitsubishi Electric Co.

H-mode conditions are suppressed by increasing the heating power. ELM/ERPs are found to be suppressed by plasma current ramp down, whereas they are enhanced by current ramp up. MHD aspect of ELM/ERP was investigated. No clear MHD features of ELM/ERP were found. However, reversal of mode rotation seen immediately after ELM/ERP suggests the temporal return to L-mode during the ELM/ERP event.

JFT-2MモードプラズマにおけるELMの特性

日本原子力研究所那珂研究所核融合研究部

松本 宏・R. J. GOLDSTON*・船橋 昭昌・星野 克道
川島 寿人・河上 知秀・前田 彦祐・的場 徹
松田 俊明・三浦 幸俊・森 雅博・中沢 一郎**
小田島和男・小川 宏明・小川 俊英・大麻 和美
仙石 盛夫・荘司 昭朗・鈴木 紀男・玉井 広史
上杉 喜彦・山内 俊彦・山本 巧・大塚 英男

(1989年2月1日受理)

JFT-2MのHモードプラズマにおいて観測される周辺振動現象(ELM/ERP)の特性について明らかにした。ELMは周辺電子密度に大きな影響を与えるが、電子温度への影響は、セパトリックス面の近傍を除くと少ないことが、ECE測定より明らかとなった。

ELMの起きる実験的条件、制御方法を明らかにし、まとめた。まず、重水素プラズマ中では、一般にELMは起きにくい、密度が低くなると起きる。また、重水素プラズマに比べ、水素プラズマ中ではELMは起きやすい。このELMは加熱入力を増すことにより、抑制できる。また、プラズマ電流をたち下げることにより抑制でき、たち上げることにより、ELMを生成できることが明らかにされた。

ELMのMHD特性を磁気プローブ信号の解析より明らかにした。

那珂研究所：〒311-01 茨城県那珂郡那珂町大字向山801-1

* プリンストン大学プラズマ物理研究所

** 外来研究員、㈱三菱電機

Contents

1. Introduction	1
2. Experimental Setups	1
2.1 JFT-2M Tokamak	1
2.2 NBI System	2
3. Experiments	2
3.1 Locality of ELM/ERP	2
3.2 Controlling Parameters of ELM/ERP	3
3.2.1 Effect of Density on ELM/ERP	3
3.2.2 Effect of Plasma Species on ELM/ERP	4
3.2.3 Effect of Power on ELM/ERP	4
3.2.4 Effect of Current Ramping on ELM/ERP	5
3.3 Analysis of B_{θ} Probe Data	6
3.3.1 MHD Analysis of H-mode Discharge	6
3.3.2 MHD Analysis of ELM/ERP	6
4. Discussions	7
5. Conclusions	8
Acknowledgement	9
References	9

目 次

1. はじめに	1
2. 実験装置	1
2.1 JFT-2Mトカマク	1
2.2 NBI加熱装置	2
3. 実験	2
3.1 ELMの局所性	2
3.2 ELMの制御条件	3
3.2.1 電子密度効果	3
3.2.2 イオン種の効果	4
3.2.3 加熱入力の効果	4
3.2.4 電流立ち下げ立ち上げの効果	5
3.3 磁気プローブ信号の解析	6
3.3.1 Hモード時のMHD解析	6
3.3.2 ELMのMHD解析	6
4. 議論	7
5. まとめ	8
謝 辞	9
参考文献	9

1.Introduction

Since the first discovery of the enhanced confinement mode, H-mode, edge localized localized phenomena named edge localized mode (ELM) in ASDEX^{1,2)}, or Edge Relaxation Phenomena(ERP) as reported on PDX³⁾ have been observed during H-mode.

This phenomena is characterized by the frequent bursts or spikes in the signal of $H\alpha/D\alpha$ emission or in B_0 magnetic probe signals. Also bursts of charge exchange neutrals and transport of impurity ions from the bulk of the plasma to the periphery are reported⁴⁾. This is called edge localized mode, because its activities are only seen in the plasma periphery. however fast growing spikes in the $H\alpha/D\alpha$ signals are becoming the definition of ELM/ERP in practical sense, and spikes seen during H-mode can be loosely called ELM/ERP. In this paper we follow this convention.

Although ELM/ERP is the very edge localized phenomena, it clearly affects the global confinement characteristics of H-mode plasma. Particle and energy confinement are deteriorated by ELM/ERP. When ELM/ERP is absent, a radiation loss or density increases very strongly resulting in a rather short termination of H-mode. A presence of ELM/ERP sometimes establish a prolonged quasi steady state H-mode.

Then, active control of ELM/ERP, not only suppressing but also creating ELM/ERP, becomes the important issue.

Also a study of ELM/ERP is very important to improve our understanding of H-mode transition physics. Recently, ELM/ERP is speculated to be a short L-mode phase. Edge plasma conditions required for H-mode maybe so marginal in ELM/ERP case, plasma can go back and forth between L and H state. Or, there must exist the self stabilizing mechanism which quickly bring the plasma back to H-mode state so quickly. For example, DIII-D experiment shows that destabilization of an ideal ballooning mode at the edge triggers giant ELM. Suppression of ELM/ERP probably mean the plasma condition at the edge becomes more favorable for H-mode.

On JFT-2M, controlling parameters of ELM/ERP were experimentally studied. Also, MHD nature of ELM/ERP were examined from the analysis of B_0 probe array measurements.

2.Experimental setups

2.1 JFT-2M tokamak

JFT-2M is a tokamak with non-circular cross section with the major radius of 1.31 m.

The maximum horizontal minor radius determined by the fixed carbon limiter is 0.35 m, and the distance from the center of the machine to the top carbon limiter is

0.55 m. It has divertor carbon tiles on the bottom floor and on the top ceiling of the vessel, so that the single null and double null divertor discharges are possible. The Maximum toroidal magnetic field is 1.4 T, and the maximum plasma current is 500 kA with a limiter configuration, and 380 kA with a divertor discharge.

2.2NBI system

JFT-2M has co-and counter- tangential beam lines. Each line injects maximum of 850 kW of the beam power in hydrogen species into the torus.

3.Experiments

3.1 Locality of ELM/ERP

Locality of ELM/ERP was studied by electron cyclotron emission measurement on JFT-2M, and it was found that the ELM/ERP activity was not clearly detected by ECE inside the separatrix surface. Emmett layer in the plasma periphery was scanned shot by shot over the edge region from 6.3 cm inside to 2.5 cm outside of the separatrix surface in the outboard midplane by changing the toroidal magnetic field. In terms of relative radial position with respect to the separatrix position, $r=a$, the range of this scan is from $r/a=0.7$ to $r/a=1.1$. In Fig.1, $H\alpha/D\alpha$ emission and the second harmonic ECE at 90 GHz are shown in each 6 radial positions. Near the separatrix, an optical thickness of the plasma is quite thin at this second harmonic, and a emission intensity is not simply proportional to a electron temperature, but it is also dependent on the electron density. Figure 1(a) shows the emission from 6.3 cm inside of the separatrix, which is 77 per cent of the minor radius position. No clear change of the signal associated with ELM/ERP can be found there. In that minor radius position, plasma should be thick enough so that the emission intensity is very weakly dependent on density. At this position, ELM/ERP is at least not the perturbation in electron temperature. Small perturbation can be observed in the ECE signal from 84 % of minor radius position shown in Fig.1(b). This layer is still optically thick. At 94 % of the minor radius position, as seen in Fig.1(c), some correlation between the fluctuation of ECE signal and the spikes of $H\alpha/D\alpha$ signal could be found, but not very clear. Signals from outside of the separatrix surface are shown from Fig(d) to (f). ELM/ERPs are now very clearly seen in the vicinity of separatrix in the scrape off layer. We must note that in the scrape off layer, the optical thickness is very thin, and the intensity of ECE signal is also dependent on density.

From these observations, ELM/ERP, not like sawtooth activities, do not accompany with the heat pulse propagation well inside the separatrix surface. Another word, its

pulsive characteristics imagined from $H\alpha/D\alpha$ signals in heat transport was not clearly found in the plasma inside the separatrix. Also, ELM activity may originate from the very edge region. Another clear observations about ELM/ERP is the sudden loss of particles near the edge region. It is always seen that FIR interferometer line averaged electron density measured vertically at $R=110$ cm (center of plasma is around $R=130$ cm) takes a dip at ELM/ERP event, whereas the central cord density does not change.

3.2 controlling parameters of ELM/ERP

Under certain experimental conditions, ELM/ERP can be suppressed or enhanced on JFT-2M. To understand the physical mechanism of ELM/ERP, a careful study of the experimental conditions which are controlling ELM/ERPs is very important. In general, ELM/ERPs are seen near the marginal H-mode conditions. For example, ELM/ERP can be seen when the heating power is just above the threshold power of the H-mode transition. And it goes away when the heating power is raised. Also, when the electron density is just above the minimum electron density necessary for H-mode, ELM/ERP appear. Or, ELM/ERP often starts appearing near the end of quiescent H-mode, just before it returns to L-mode. Detailed measurements of periphery are necessary to find the common features among these conditions which were not possible on JFT-2M. However, in the following section, experimental conditions controlling ELM/ERPs on JFT-2M in the single null divertor configuration will be cataloged.

3.2.1 effect of density on ELM/ERP

There is a minimum electron density necessary for H-mode transition on JFT-2M. Just above this density, we usually see ELM/ERP during H-mode. Figure 2 shows the low electron density and ELM/ERP case. In the figure, ECE signal from 90 % of the minor radius position, one turn loop voltage, stored energy determined from the diamagnetic measurement, total radiation loss, line averaged electron densities vertically measured at two cords showing the broadness of the density profile, the ratio of these two line averaged electron density, $H\alpha/D\alpha$ signal and neutral beam injection power are shown from the top to the bottom. Here, the effect of ELM/ERP on the evolution of electron density and radiation loss is very clear. Radiation loss is kept below the level of L-mode-pre-transition phase during the H-mode. Electron density profile becomes broad compared with that of L-mode phase, but the increase of electron density during H-mode is very mild.

In the same series of the experimental runs, ELM/ERPs were clearly suppressed simply

by raising the density. Figure 3 show the higher electron density case with very similar discharge conditions and even smaller heating power. No ELM/ERP are seen in this case, and the increase of radiation loss and the electron density is much stronger than the low density case. Both cases are hydrogen beam injection into deuterium plasma. Comparing two shots, power deposition into the peripheral region in the lower density case is not smaller than that of high density case and edge electron temperature from ECE is even higher than that of high density case. Also, in this deuterium plasma case, ELM/ERPs are usually seldom seen except this low density case, and near the end of long H-mode phase just before it returned to L-mode due to the increased radiation loss. Even, when the heating power is small and just above the threshold power ELM/ERP do not appear, provided the electron density is high enough.

3.2.2 effect of plasma species on ELM/ERP

On JFT-2M, hydrogen plasma is more susceptible to ELM/ERPs compared with deuterium plasma. Figure 4 shows the hydrogen beam injection into hydrogen plasma case with almost similar operational conditions with the case of Fig.3 where deuterium plasma was used. In both cases, beam injection power was about 670 kW, and ELM/ERP appear in hydrogen plasma case. This isotope effect could be partly due to the strong effect of heating power on ELM/ERP in hydrogen plasma which will be mentioned in the next. In this hydrogen plasma case, the NB heating power was only 100 kW above the H-mode threshold heating power. Whereas the threshold heating power in deuterium plasma of Fig.3 was 340 kW. Both threshold powers are higher than the best cases because Ti-gettering were not employed in both cases.

3.2.3 effect of power on ELM/ERP

Effect of heating power is clearly seen especially in hydrogen plasma. In hydrogen plasma, ELM/ERP is seen when the heating power is near the H-mode threshold power no matter high the electron density is raised. Two hydrogen plasma discharges with low heating power and high heating power are compared in Fig. 5 and in Fig. 6. NB injection heating power is 660 kW in case of Fig. 5 and 1400 kW in case of Fig.6. When the heating power is small, small and frequent ELM/ERP appear and increase of radiation loss and electron density is small during H-mode. Note that energy content of plasma is almost doubled from L-mode to H-mode, which is not always the case on JFT-2M, especially with deuterium plasma cases. When the heating power is high, ELM/ERP do not show up, and increase of radiation loss is such strong that plasma stored energy decrease in later phase of H-mode.

3.2.4 effect of current ramping on ELM/ERP

Effect of plasma current ramping on ELM/ERP was clearly found in the course of the current ramping experiments on JFT-2M with single null divertor configuration and hydrogen neutral beam injection into hydrogen plasma. First, plasma current was ramped up at the ramping rate of 350 kA/s and the case is shown in Fig.7. In the figure, $H\alpha/D\alpha$ signal, plasma current, loop voltage, radiation loss, line averaged electron densities at the central and peripheral cord, ratio of these line averaged electron density, ECE at 90 GHz from the periphery, radial position of this ECE emission layer normalized by the minor radius, and the neutral beam injection power are shown from the top to the bottom. In this case, the first H-mode transition takes place at 730 ms, and the second further transition takes place at 760 ms. Broadness of the electron density profile shown by the ratio of two line averaged electron density, $\bar{n}_e(r=21\text{ cm})/\bar{n}_e(r=7\text{ cm})$ is one of the good measure of the transition state. It clearly shows the broadening of the profile by two steps. Similar traces are shown in Fig.8 where the plasma current was ramped down at the same ramping rate. In this case, ELM/ERPs are very much suppressed compared with the ramping up case. H-mode transition in this shot took place at 725 ms. Spikes in $H\alpha/D\alpha$ in the initial phase of H-mode are suppressed by 750 ms, and the radiation loss starts increasing more strongly than the H-mode phase with current ramp down in the previous figure. But, the H-mode state terminates rather shortly at 830 ms, and then radiation loss starts declining and the density profile begins to shrink.

Plasma current was ramped down and up more steeply at the rate of 700 kA./s. Time evolutions of the same plasma parameters as Fig.7. and 8 are shown in Fig.9 with ramping down and up case, and in Fig.10 with ramping up and down case. In case of Fig.10, H-mode which started from 725 ms lasts until the end of NB pulse. During the ramp up phase, central line averaged electron density increases, but the radiation loss decrease due to ELM/ERP activity. In case of Fig.10, H-mode starts from 720 ms and ELM/ERP activity is suppressed 30 ms after the start of ramping down. And H-mode terminates rather early, at 870 ms. In both cases it is clearly shown that during the ramping up period, ELM/ERPs are enhanced, and during the ramping down phase, ELM/ERPs tend to be suppressed.

It is worth while taking notice of the fact that H-mode is taking place during the strong current ramping down phase when the loop voltage is negative. Here, loop voltage is the average of inner and outer flux loop voltage, and the effect of the plasma movement for this loop voltage measurement was almost negligible. This should clearly contradicts the physical model of H-mode proposed by Bishop⁵⁾.

3.3 Analysis of B_θ probe data

It is natural to expect that ELM/ERP has a MHD activity nature, since the effect of current ramping is very clear. It could be a surface kink type MHD, due to the surface plasma current density. Then it is very important to study the MHD nature of H-mode or ELM/ERP. 12 arrays of B_θ probe data were analyzed to estimate the MHD mode structure of ELM/ERP. B_θ probes mainly detects magnetic fluctuations caused by scrape off layer current fluctuations. Although, in many cases, it reflects MHD fluctuations of main plasma especially, in low n and m number modes. On JFT-2M, array of 12 B_θ probes shown in Fig. 11 were installed only in one toroidal position, and n number can not be determined.

3.3.1 MHD analysis of H-mode discharge

Single null divertor discharge of shot number 39748 whose shot data are shown in Fig. 2 was chosen as an example of MHD analysis from B_θ probes poloidal arrays. First, we show the contour plot of probe signal intensity in time and poloidal angle. Horizontal axis is time, and vertical axis is the poloidal position of probes in angle, starting from the inside mid-plane to top, outer mid-plane, bottom, and the inner mid-plane. $m=2$ mode rotates in the electron diamagnetic direction at a frequency of 4.7 kHz during Ohmic phase. Co-injection neutral beam starts from 700 ms. The frequency of this rotational does not change within ± 0.1 kHz after the onset of beam injection. This may suggest that the toroidal rotation of the surface where this fluctuation originates does not change more than 800 m/s by the injection of this 1 MW neutral beam. As can be seen from Fig.12, H-mode transition takes place around 734 ms. Figure 13 shows the same contour plot from 732 ms to 734.5 ms. At the transition, the $m=2$ mode suddenly changes the direction of rotation, and then the amplitude of this oscillation dies down. This could be due to the sudden change of toroidal rotation speed in the edge or the sudden change of the poloidal rotation.

3.3.2 MHD analysis of ELM/ERP

Fig. 14 shows the magnetic probe data, ECE signal from the periphery, peripheral cord line averaged electron density and $H\alpha/D\alpha$ signal around the ELM/ERP event. ELM/ERP takes place just before 756 ms and the ECE signal and line averaged electron density in the periphery take a dip at that instance. A peak in $H\alpha/D\alpha$ signal is seen around that time, although it has only 1 ms of time resolution and is not appropriate to match the

timing of ELM/ERP. ECE and density information in this figure have 0.2 ms of the resolution. At the onset of ELM/ERP, strong $m=1$ mode fluctuation appear in magnetic probe signals. Signal BP01 and BP14 are separated by almost 180 degree in poloidally, and they are out of phase. about 1 ms later another mode of fluctuation appear. A structure of this fluctuation can be seen from the contour plot of magnetic probe signals in Fig. 15. It is $m=2$ and the rotation would be in the ion diamagnetic direction. This mode is rather strongly localized in the bad curvature region, and this localization must be even stronger on the separatrix surface, since the distance between the separatrix surface and the probe of low field side in the midplane is more than two times as large as that of high field side.

The similar analysis was made with the current ramping shot where plasma current was first ramped down from 700 ms and then ramped up from 750 ms at the ramping rate of 1.6 MA/s. Co-directional neutral beam was injected from 700 ms to 900 ms. H-mode transition took place around 730 ms during the strong ramping down phase. Three ELM/ERPs from 790 ms to 810 ms, near the end of ramping up are show in Fig. 16. Signals of nine B_0 probes, ECE from the periphery, line averaged electron density in the periphery, and $H\alpha/D\alpha$ signal are shown in the figure from the top to the bottom. Here, $H\alpha/D\alpha$ signal has only 1 ms of the time resolution while ECE and density information in this figure have 0.2 ms of the resolution. Timing of ELM/ERP could be best determined from ECE signal with 0.2 ms of accuracy. In this ramping case, we can not find any MHD fluctuations which precede or synchronize with ELM/ERPs. We rather find the fluctuation which follows ELM/ERP. Structures of these fluctuations are shown in Fig. 17 and in Fig.18. Figure 17 show the contour plot of probe signals from 795 ms to 800 ms. $m=1$ mode is not seen at the timing of ELM/ERP, and the $m=2$ mode rotating in the ion diamagnetic direction is very shortly seen on the bad curvature region. It is more clearly shown in Fig. 19 where contour of 800 ms to 805 ms is plotted.

4. Discussions

ELM/ERPs dumps n_e near the edge, but it does not affect electron temperature very much inside the separatrix surface. Right after ELM/ERP, η_e or probably η_i are quite enhanced near the edge. This may suggest that the H-mode is not directly controlled by the mixing length in the edge.

Reversal of mode rotation, and enhanced $H\alpha/D\alpha$ emission associated with ELM/ERP

suggest a temporal return to L-mode triggered by ELM/ERP. More precisely, ELM/ERP could be defined as fluctuations or small change of the plasma condition which temporarily destroys the H-mode condition in the edge. In a broader sense, ELM/ERP event include the short L-mode phase when H_{α}/D_{α} emission is strongly enhanced. Then, an important question is what kind of instability or mode happens. Certainly, MHD instabilities are good candidates. The experimental observation in JFT-2M that ELM/ERPs are strongly affected by the current ramping suggests MHD activity associated with the current gradient in the edge. Considering its very fast time scale and low m number nature, it could be an ideal MHD mode. However, no unique MHD signal of ELM/ERP can be found in JFT-2M. In case of current ramping experiment, any clear MHD activities cannot be detected by B_{θ} probes at ELM/ERP. It is more likely that there exist several mechanisms responsible for ELM/ERP. Good example is the observation in DIII-D, the excessive pressure gradient invoking the ideal ballooning instability in the steep density gradient region triggers a giant ELM/ERP⁶⁾. Probably it is giant because it happens at the very steep pressure gradient, and the break of transport barrier associated with the ELM/ERP event result in release of huge particle and energy from the edge. However, most of ELM/ERP in JFT-2M happen near the power threshold, and they are suppressed when the heating power is raised, which are contrary to DIII-D result. This suggest most of ELM/ERP in JFT-2M are not like giant ELM/ERPs, and they happen far below the ideal ballooning limit.

Most of the experimental conditions favorable for ELM/ERP are at the same time unfavorable conditions for H-mode transition. If the edge plasma parameters well satisfy the H-mode conditions, a small perturbation caused by MHD activity or other instability will not destroy the H-mode conditions. And certain plasma parameters also control this MHD activities or instabilities in the edge. Therefore, if we can suppress ELM/ERP by changing certain plasma parameters, it is not very clear if the plasma was brought into more favorable state for H-mode or the edge instability which was triggering ELM/ERP was simply stabilized. This is well illustrated by the case of current ramping. ELM/ERPs are very much affected by the ramping suggests they are controlled by the current gradient at edge. At the same time, we can see H-mode does not require edge ohmically driven current and in general not too sensitive to $j(r)$ near the edge, because H-mode state is maintained or transition can be seen when the surface voltage V is negative or positive due to the strong current ramping down or up.

5. Conclusions

1. ELM/ERPs dump particles in the edge, but edge electron temperature except just

near the separatrix is not very much affected by ELM/ERP.

2. ELM/ERPs occur near the power and ne thresholds and this suggests regular ELM/ERPs in JFT-2M are not associated with a maximum in the pressure gradient at the edge.
3. ELM/ERPs affected by $V_1(\text{edge})$ suggests they are associated with the current gradient at edge. Incidentally, it was indicated that H-mode does not require edge ohmically driven current, and in general not too sensitive to $j(r)$ near edge.
4. Enhanced H_α/D_α emission, and following reversal of mode rotation seen at ELM/ERP suggest the temporal return to L-mode during the ELM/ERP event.

Acknowledgements

The authors are very grateful to the members of the JFT-2M operation group lead by Mr. K. Suzuki for their excellent technical contributions. They are also indebted to Drs. S. Mori, K. Tomabechi, M. Yoshikawa, and M. Tanaka for their continuous encouragement.

REFERENCE

1. F. Wagner et al., Phys. Rev. Lett. 49, 1408 (1982).
2. F. Wagner et al., J. Nucl. Mater. 121, 103 (1984)
3. S. M. Kaye et al., J. Nucl. Mater. 121, 115 (1984)
4. D. Hill et al., Nucl. Fusion 28, 902 (1988)
5. C. M. Bishop, Nucl. Fusion 26 (1986) 1063
6. P. Gohil et al., Phys. Rev. Lett. 61, 1603 (1988)

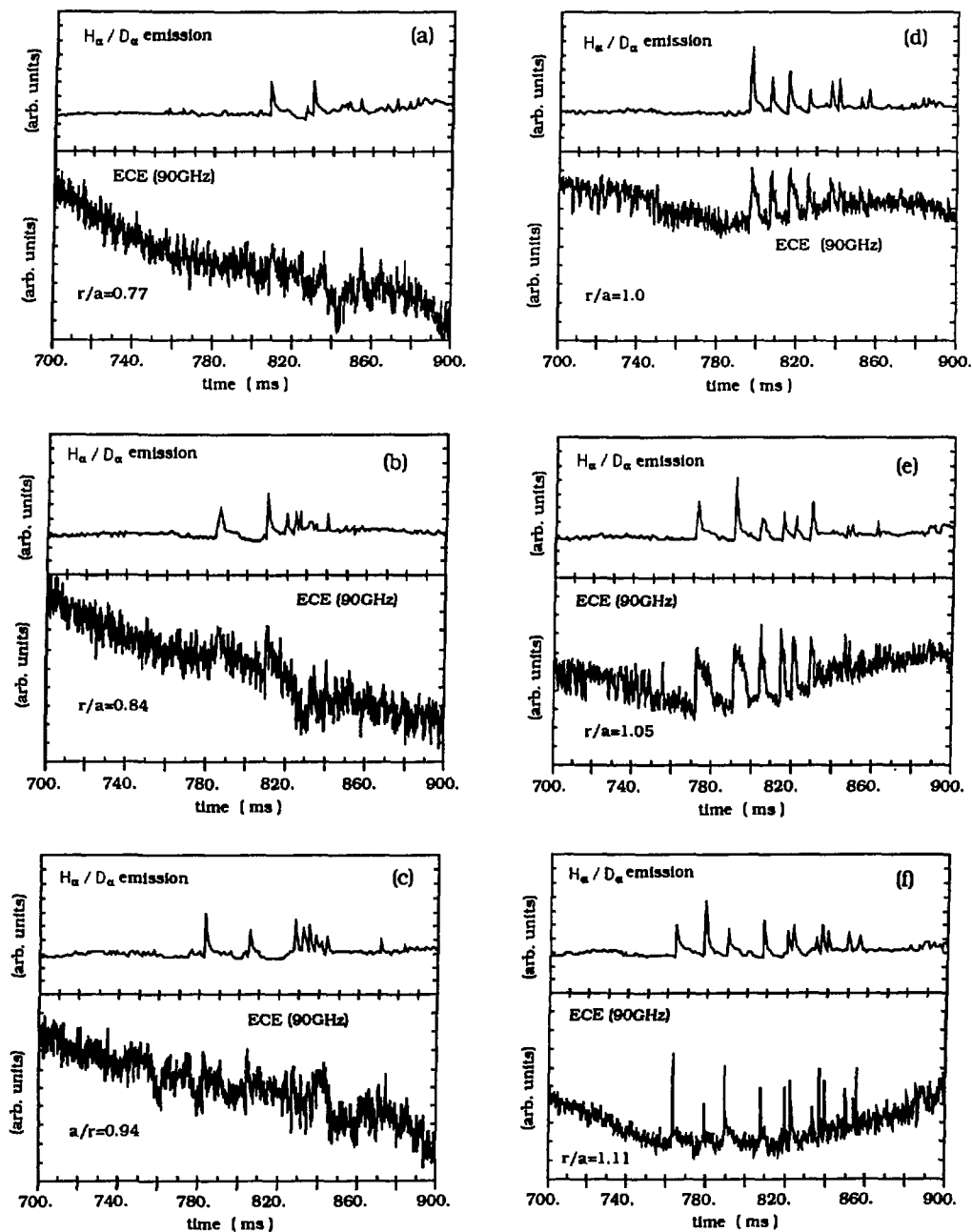


Fig.1 H_{α}/D_{α} emission and edge electron temperature at various radial location near the separatrix surface showing the effect of ELM/ERP on edge electron temperature.

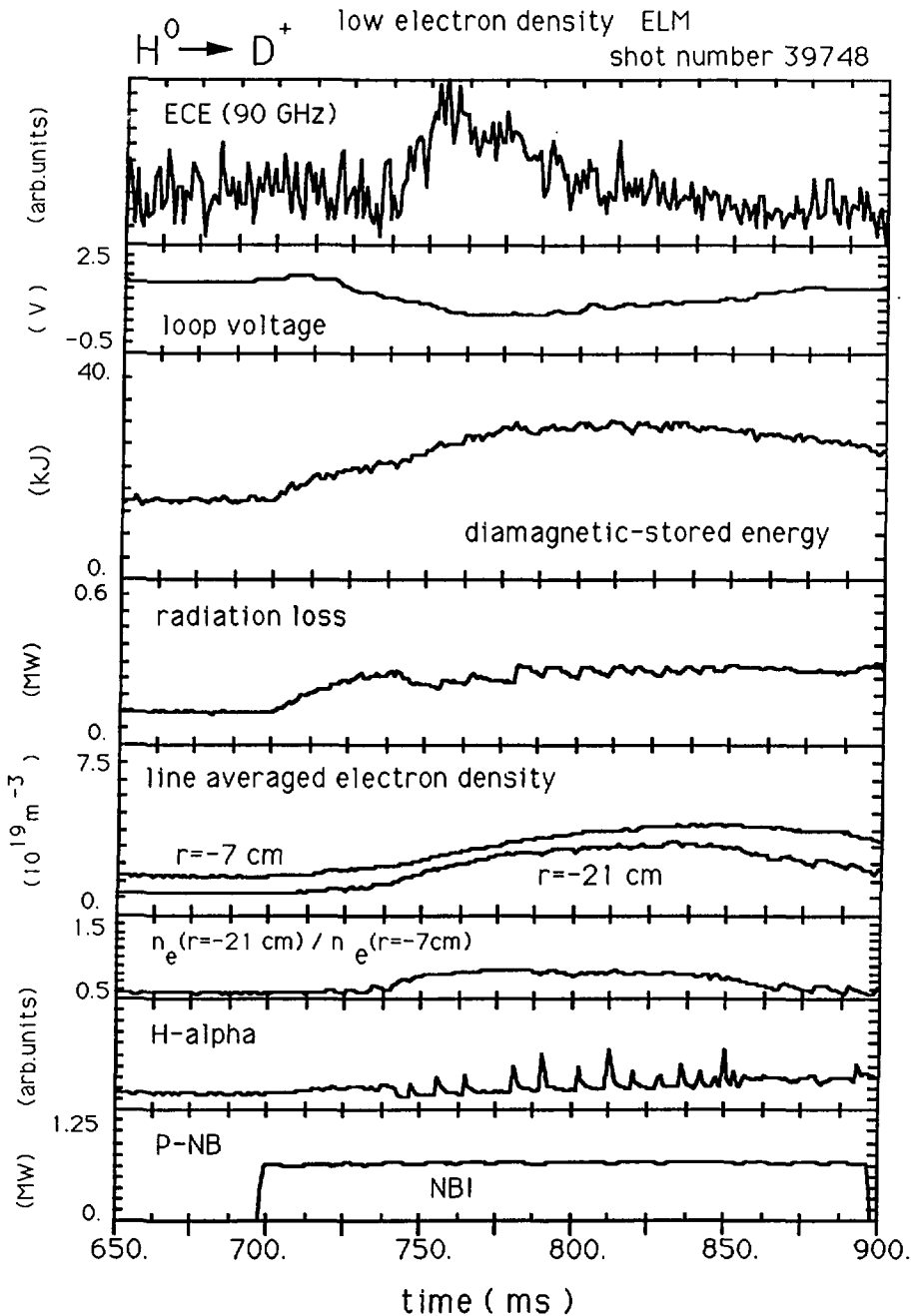


Fig.2 Time evolutions of edge electron temperature, loop voltage, diamagnetic stored energy, total radiation loss, line averaged electron densities at two vertical chord through $r=7, -21$ cm, ratio of the peripheral to the central chord line average electron density showing the broadness of the density profile, H_{α}/D_c emission, and neutral beam injection power for the case of hydrogen beam injection into low density deuterium plasma.

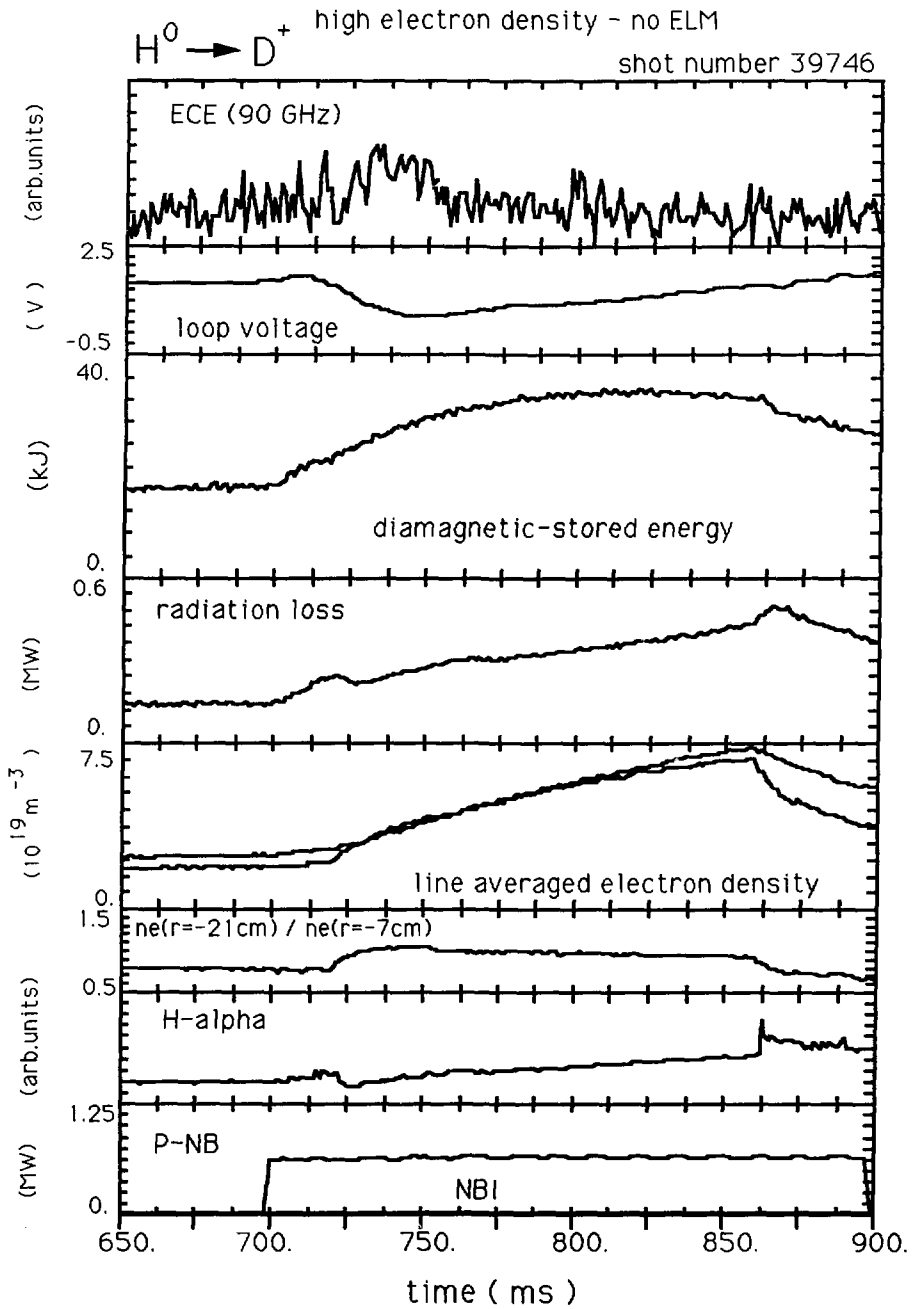


Fig.3 Similar traces of $H^0 \rightarrow D^+$ high density case when ELM/ERP are suppressed.

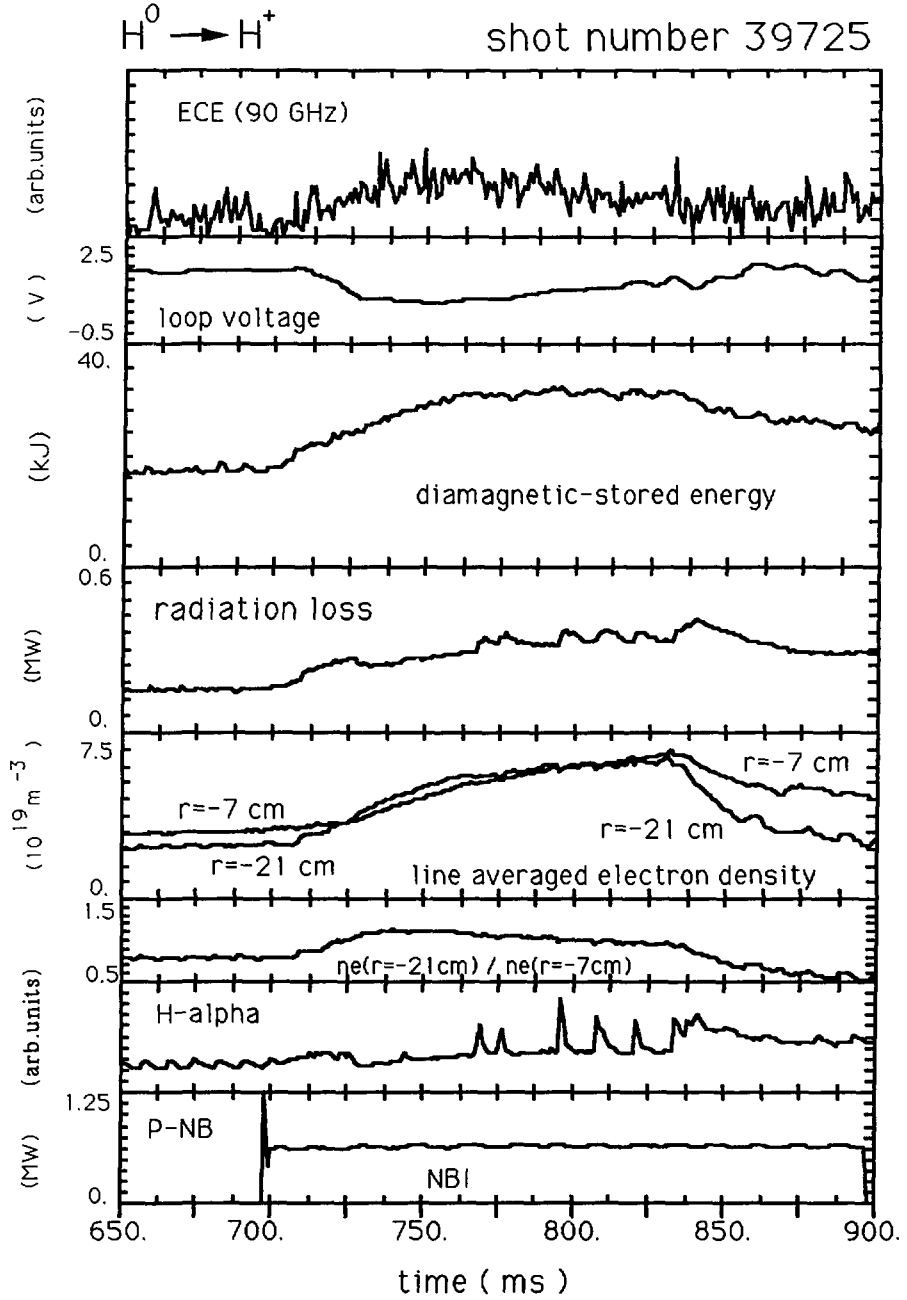


Fig.4 $H^0 \rightarrow H^+$ discharge with the same discharge conditions of Fig.3 except the plasma ion species showing ELM/ERP in hydrogen plasma case.

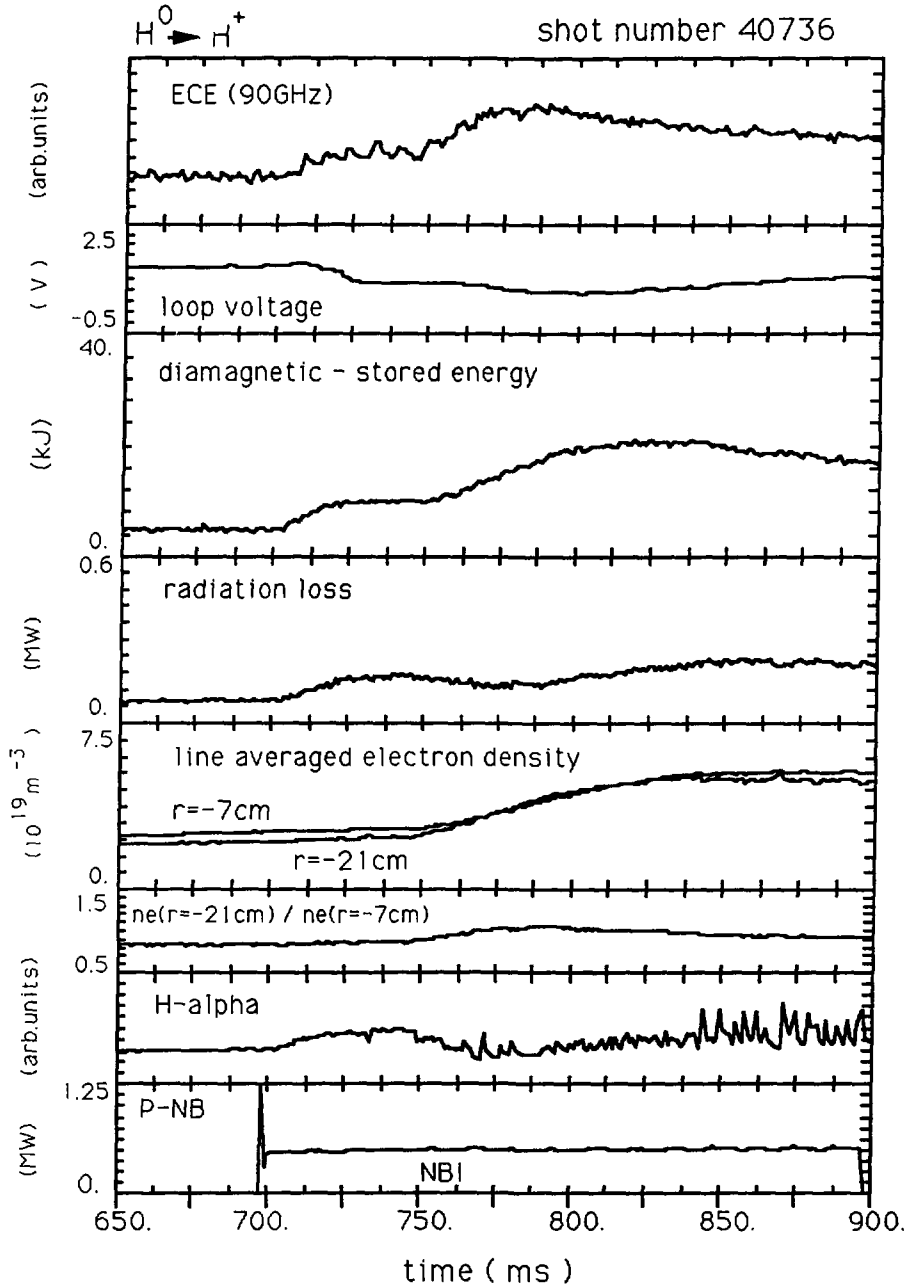


Fig.5 $H^0 \rightarrow H^+$ discharge with the heating power of just above the threshold power for H-mode resulting ELM/ERP activities .

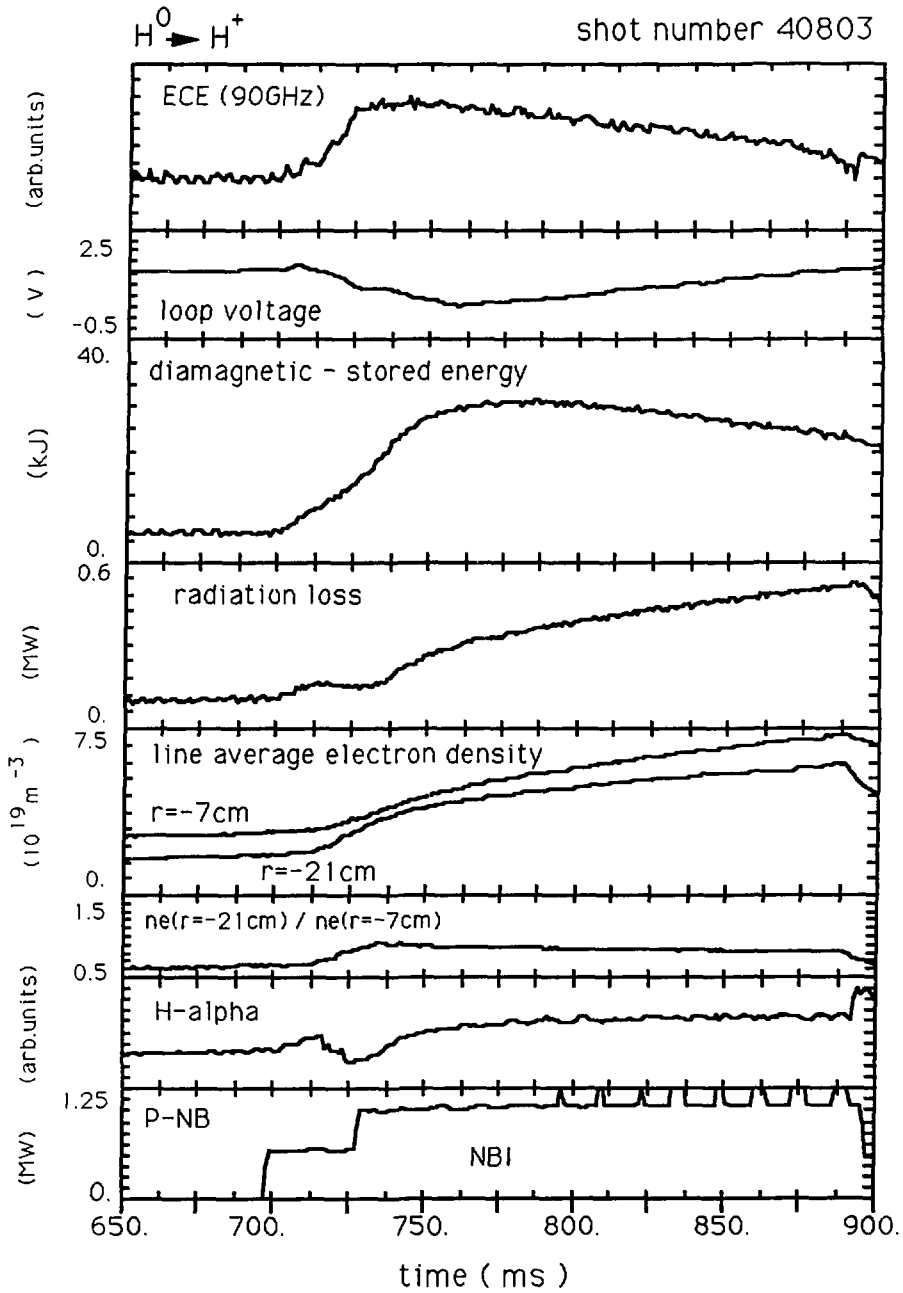


Fig.6 Heating power was raised from the case of Fig.5 with other discharge conditions identical. Now ELM/ERP are suppressed.

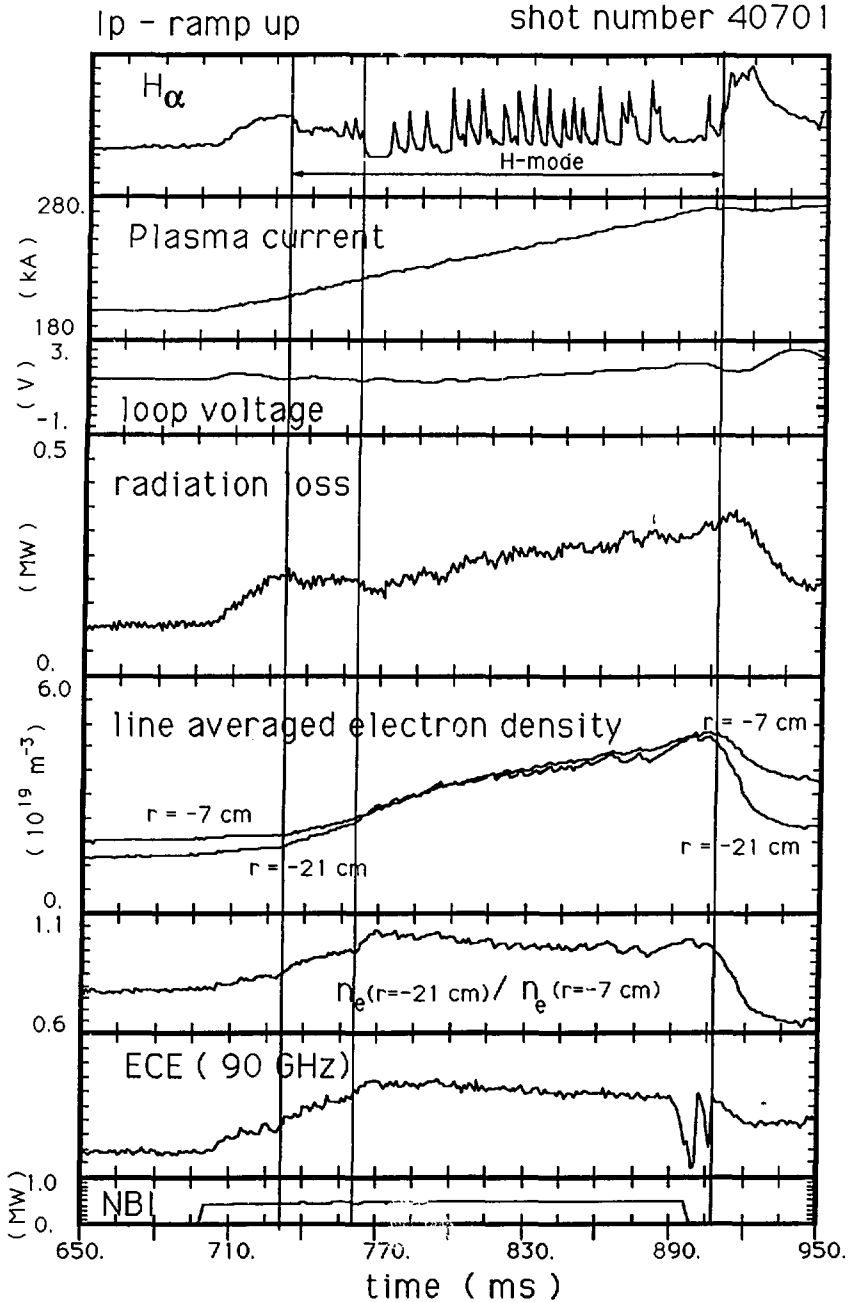


Fig.7 Hydrogen beam injection into hydrogen plasma during the current ramping up. Enhanced ELM/ERP activities are seen.

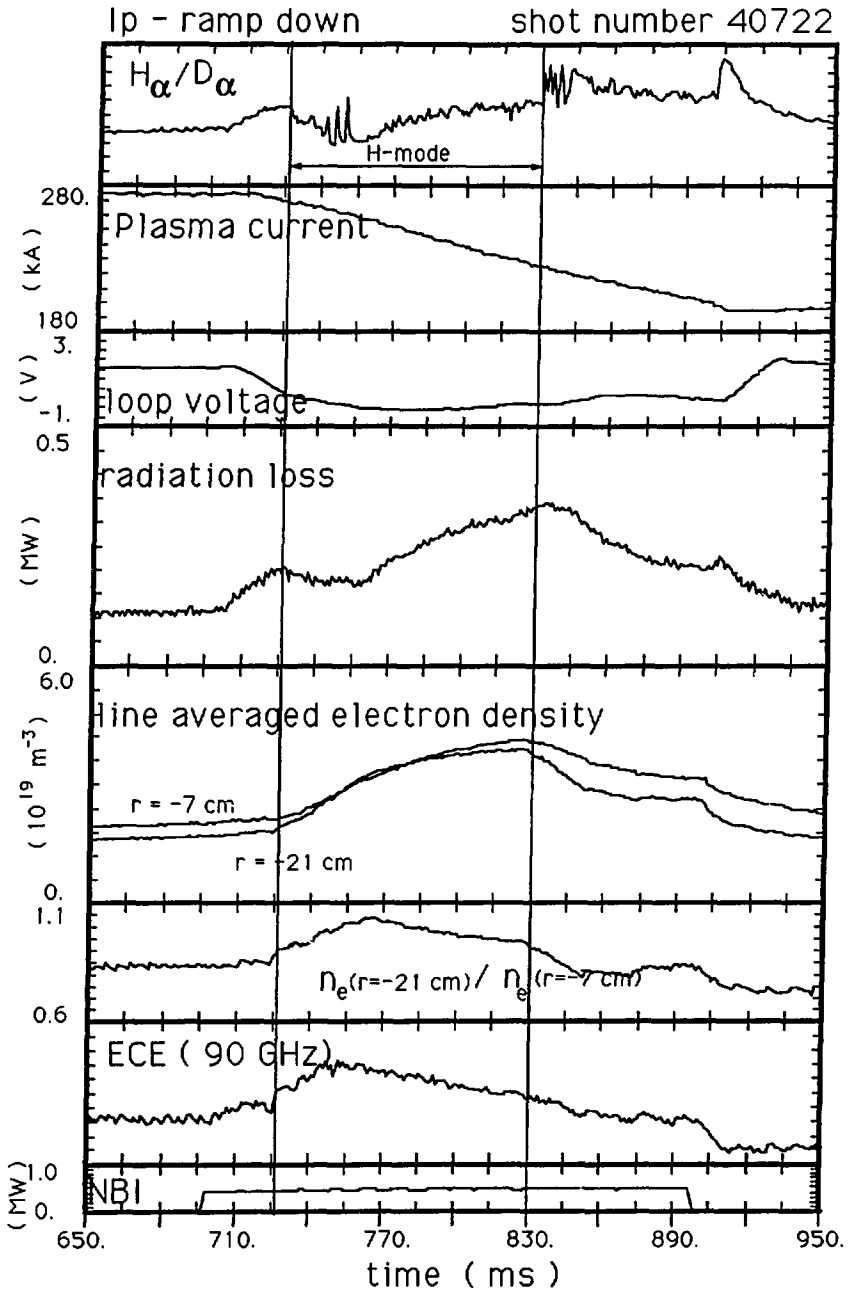


Fig.8 $H^0 \rightarrow H^+$ discharge with current ramp down. Compared with ramp up case, ELM/ERP is very much suppressed, although the duration of H-mode is short.

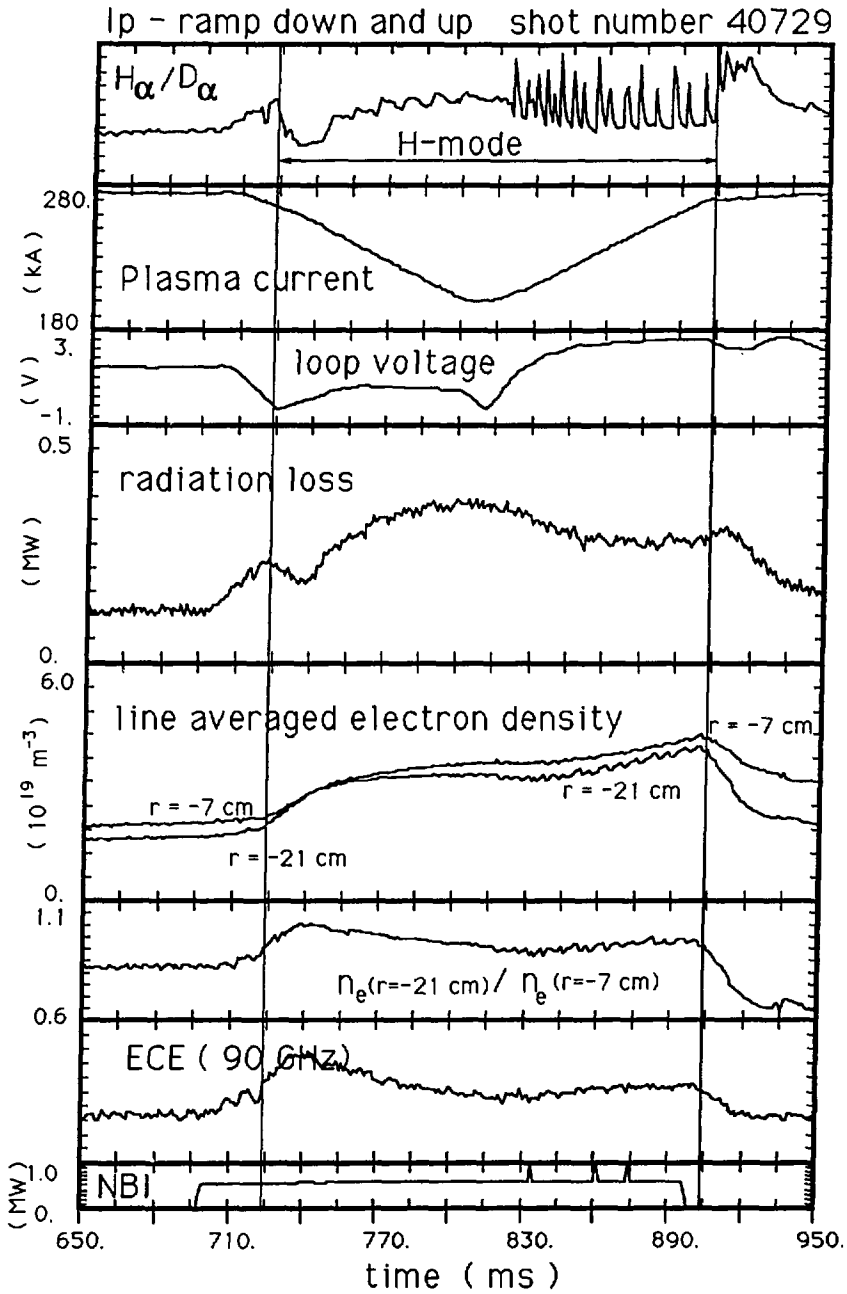


Fig.9 Current ramp down and up case. ELM/ERPs are suppressed during the ramp down phase and they are enhanced during the ramp up phase.

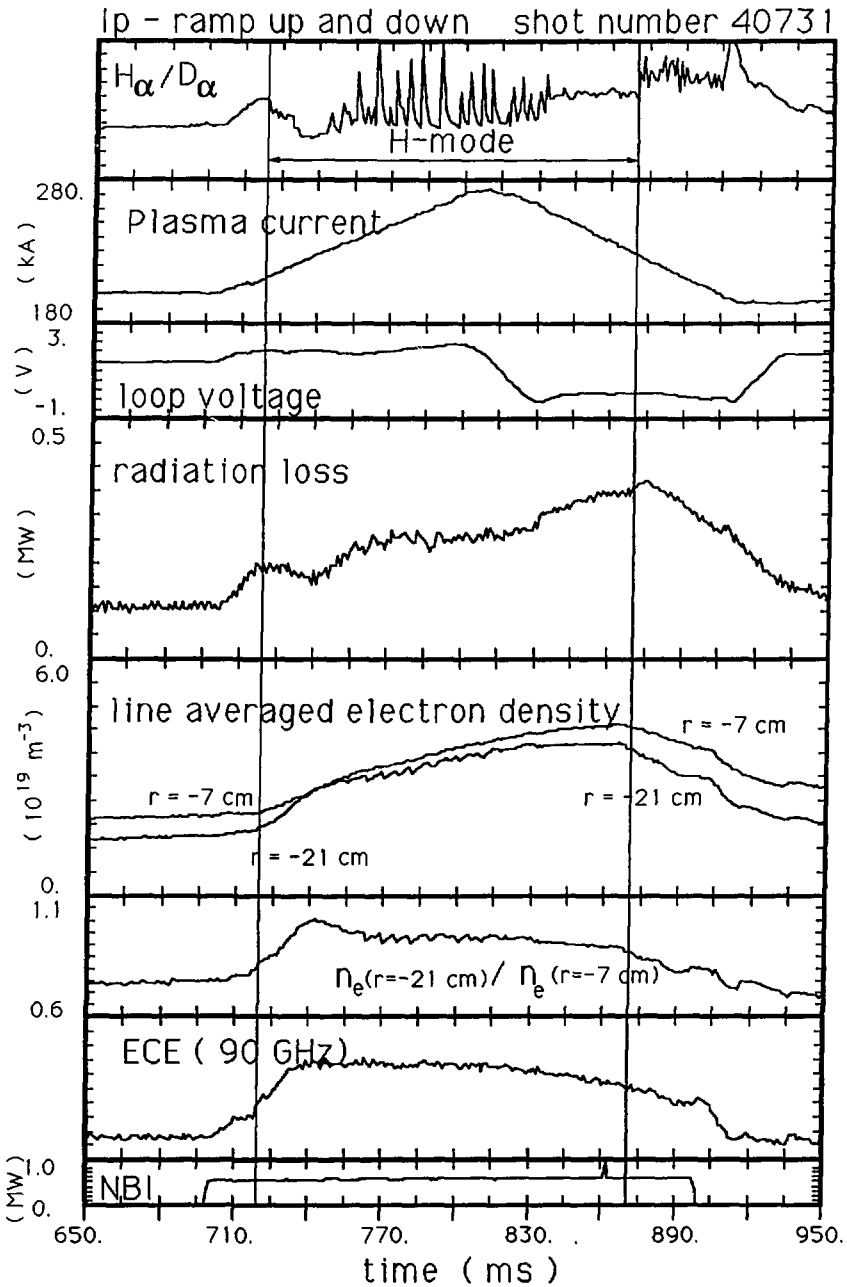


Fig.10 Current ramp up and down case. ELM/ERP s are suppressed in the latter part of H-mode during the ramp down phase, although H-mode terminates rather early.

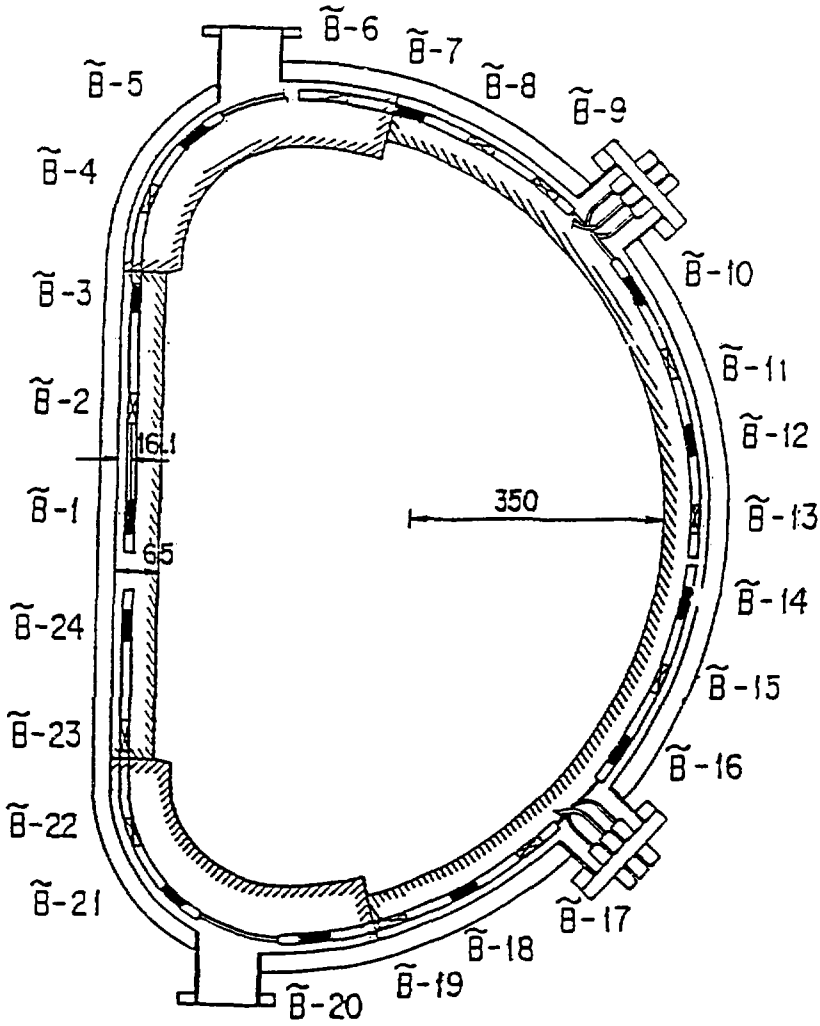


Fig.11 Arrangement of \tilde{B}_0 probe arrays in JFT-2M.

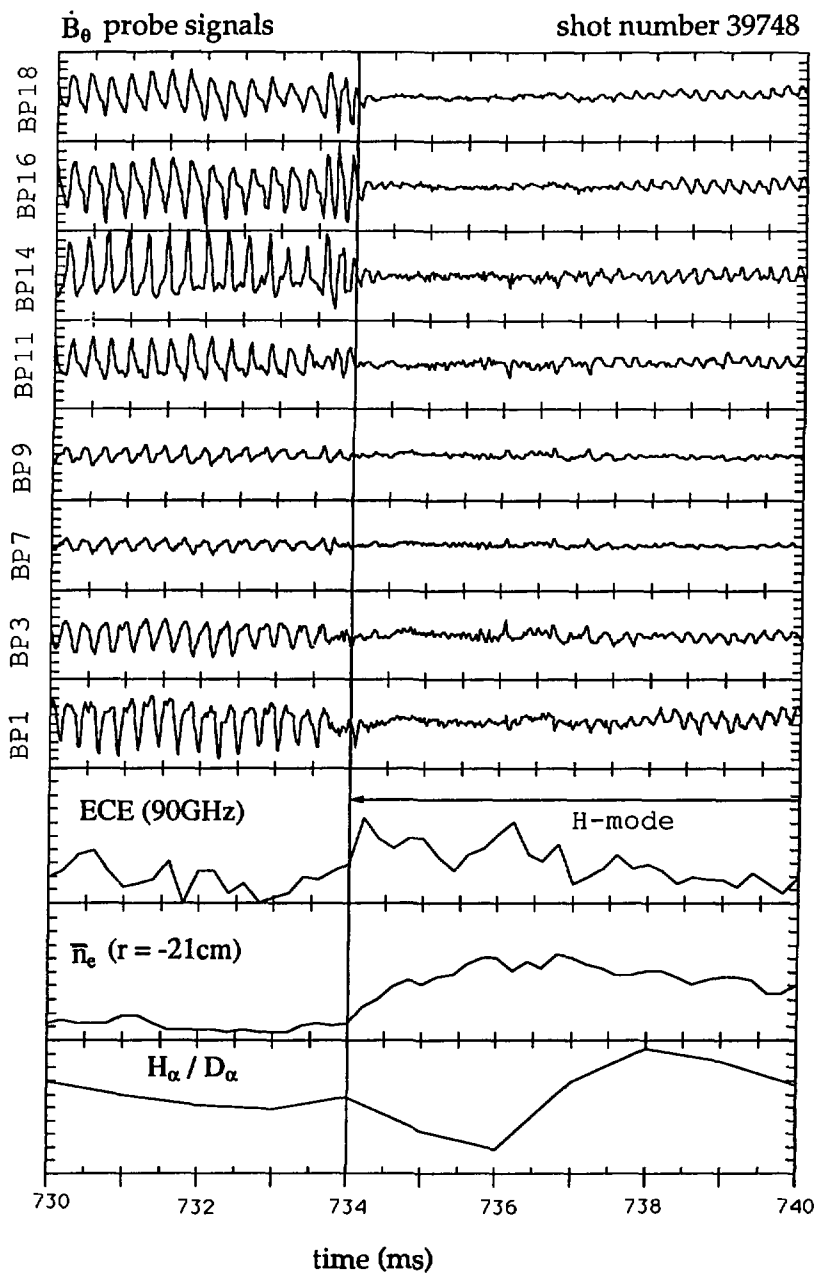


Fig.12 L-H transition phase of the shot shown in Fig.2 was blown up. Signals of 8 \tilde{B}_0 probes whose location can be identified by Fig.11, edge electron temperature, peripheral chord line average line density, and H_α/D_α emission are shown.

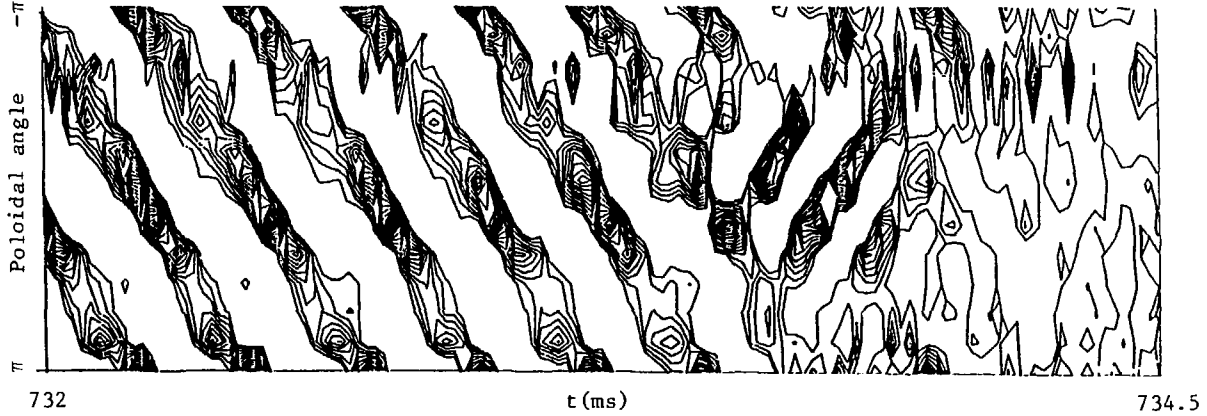


Fig.13 The contour plot of magnetic probe signal intensity in time and poloidal angle. Vertical axis is the poloidal angle coordinate with 0 at the outer midplane, $-\pi/2$ at the top of the vessel, and $\pi/2$ at the bottom of the vessel. Horizontal axis is time. $m=2$ mode is rotating in the electron diamagnetic direction first, and the sudden change of the rotational direction is seen at the transition following the suppression of the $m=2$ mode.

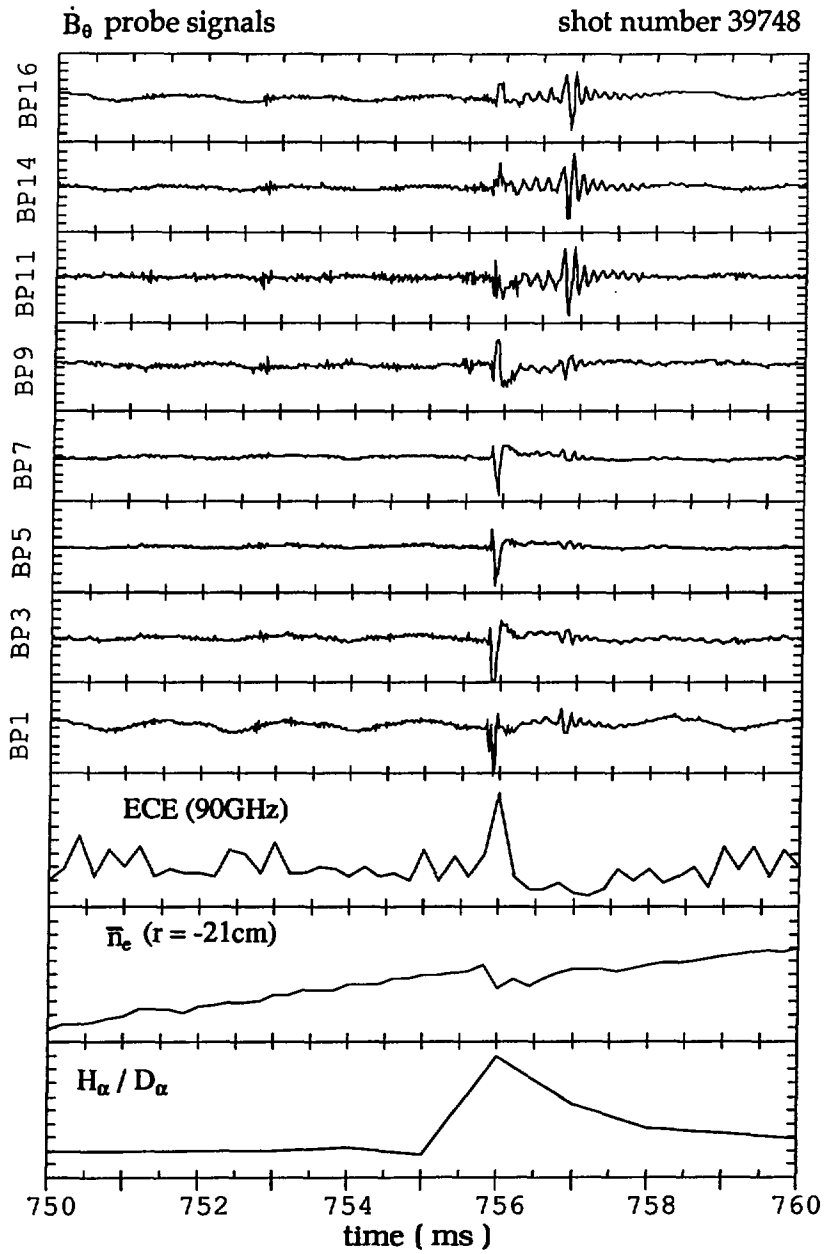


Fig.14 Similar time evolutions of signals as Fig.12 showing ELM/ERP around 756 ms.

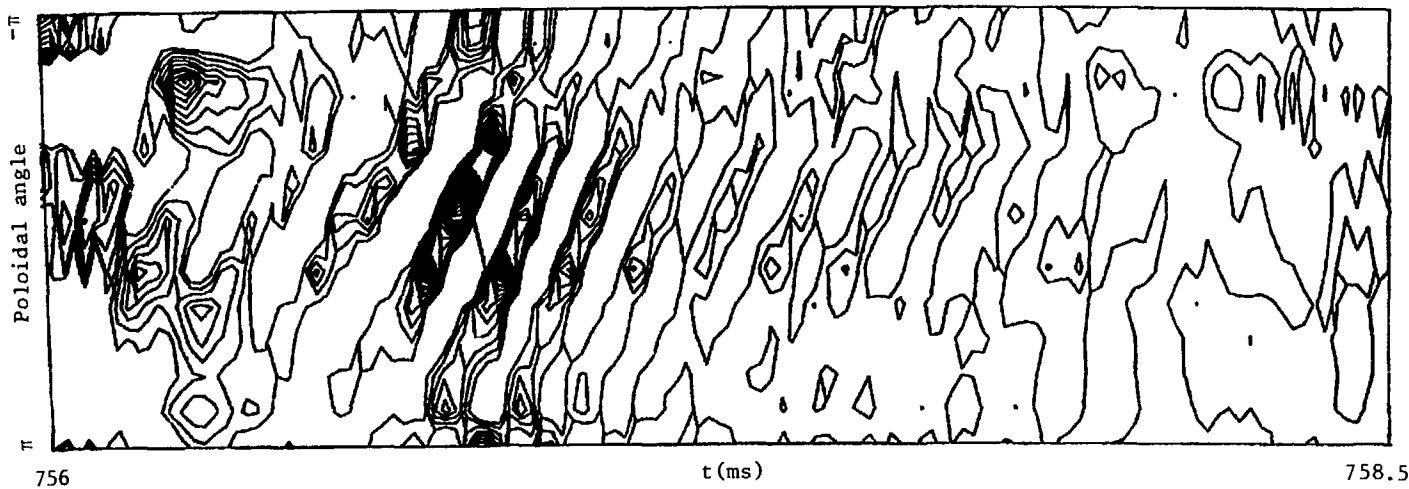


Fig.15 Magnetic contour surface plot similar to Fig.13 around an ELM/ERP event shown in Fig.14.

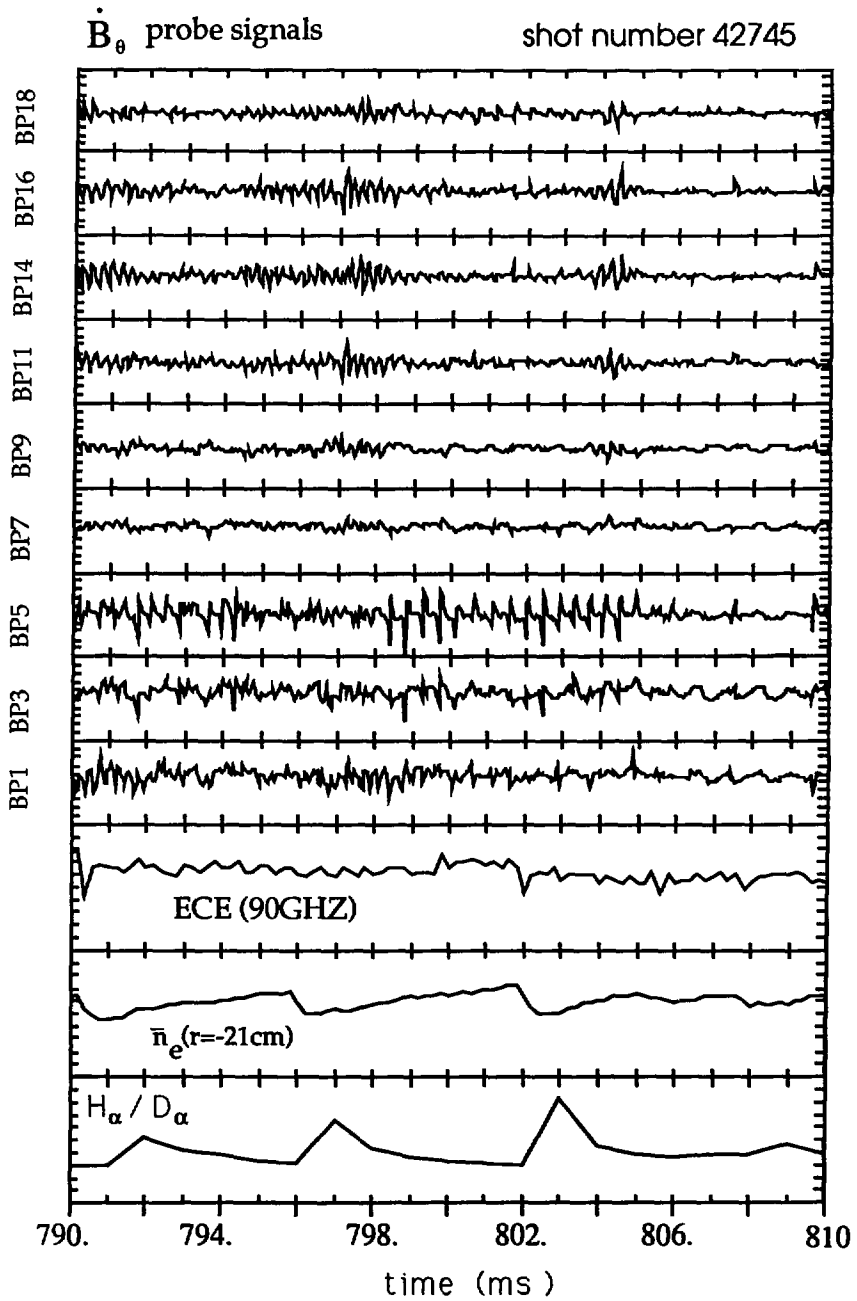


Fig.16 Signals of 8 \dot{B}_θ probes, edge electron temperature, peripheral chord line average line density, and H_α/D_α emission near the end of strong current ramp up phase showing three ELM/ERPs.

Shot # 42745

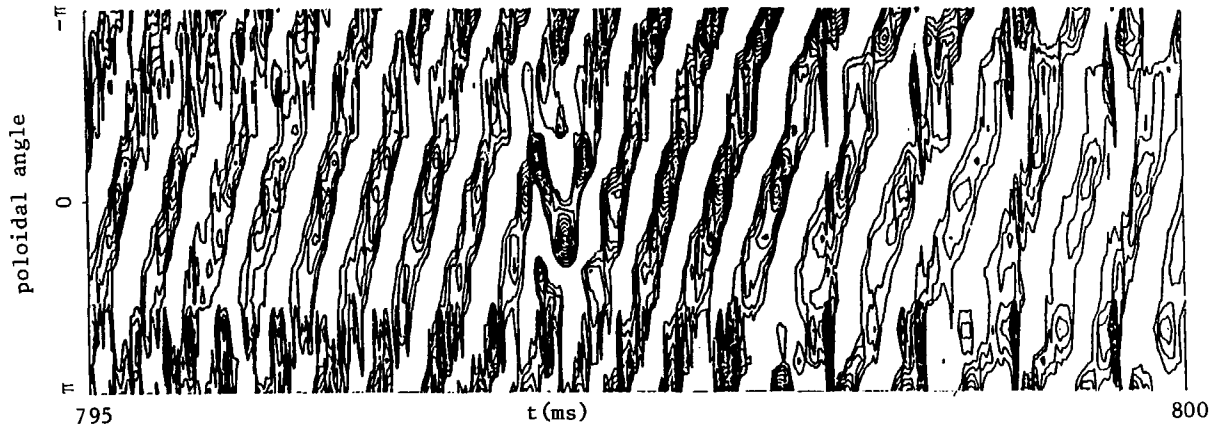


Fig.17 Magnetic contour surface plot similar to Fig.13 from 795 ms to 800 ms.

Shot # 42745

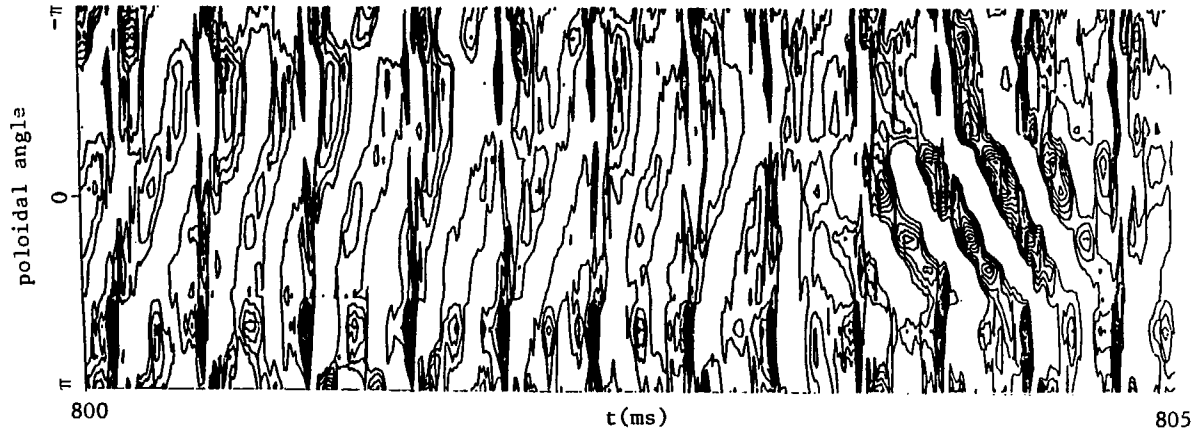


Fig.18 Magnetic contour surface plot similar to Fig.13 from 800 ms to 805 ms.